

Supporting Information for

Using Engineered Single-Chain Antibodies to Correlate Molecular Binding Properties and Nanoparticle Adhesion Dynamics

Jered B. Haun^{†,}, Lauren R. Pepper[†], Eric T. Boder[§] and Daniel A. Hammer^{†,‡}*

MATERIALS AND METHODS

Verification of VIII scFv Specificity for VCAM-1. EBY100 yeast transformed with pCTVIII plasmid were grown overnight in 3 ml SD-CAA (20.0 g/L dextrose, 6.7 g/L yeast nitrogen base, 5.0 g/L casamino acids, 5.4 g/L Na₂HPO₄, 7.46 g/L NaH₂PO₄) cultures at 30°C, followed by induction of 10⁷ cells in 3 ml SG-CAA for 24 hours at 20°C. VIII scFv expression was then assessed by flow cytometry using functional (VCAM-1/Fc followed by Alexa 488-conjugated protein G, each at 10 µg/ml) and indirect (anti-c-myc antibody at 7 µg/ml followed by RPE-conjugated goat anti-mouse IgG₁ antibody at 10 µg/ml) assays. Incubations were performed for 1 hour, with the primary reaction at room temperature and secondary at 4°C. All washes were performed with three rounds of centrifugation and resuspension in ice-cold PBS containing 1% BSA (PBS⁺). Fluorescence was assessed by flow cytometry using a FACsCalibur cytometer (BD Biosciences). Controls included secondary reagent only.

Biotinylation of 4-4-20 Antibody. Unmodified 4-4-20 antibody was first purified to remove BSA using a 1 ml HiTrap protein G affinity column (GE Healthcare). The antibody was added to the column

at 1 ml/min, washed for 10 min with PBS and eluted with 0.1 M glycine-HCl (pH 2.7). Elution was monitored by absorbance at 280 nm, and 0.5 ml fractions were collected into tubes containing 50 μ l of 1 M Tris-HCl (pH 9) to balance the acidic elution buffer. Peak fractions were concentrated and buffer exchanged to PBS using an Amicon Ultra-4 centrifugal concentrator. The purified solution (900 μ g antibody/ml by micro-BCA) was then biotinylated by addition of sulfo-NHS-LC-biotin (Thermo Fisher) at 20-fold molar excess for 1 hour at room temperature. Following biotinylation, free biotin was removed using Zeba desalting spin columns (Thermo Fisher) and the sample was concentrated using an Amicon Ultra-4 centrifugal concentrator, yielding a 350 μ l solution at approximately 2 mg/ml.

Particle Characterization. Receptor surface density on 210 nm particles was assessed by ELISA using HRP-conjugated probes. These HRP probes included anti-c-myc antibody (scFv), anti-mouse κ light chain (4-4-20 antibody), and Neutravidin (biotinylated BSA), and each was used at 10 μ g/ml final concentration with 1 ml of functionalized particles that were pooled from peak chromatography elution fractions. After reaction for 1 hour at room temperature, samples were purified using a second round of size-exclusion chromatography and prepared for ELISA by adding to opaque 96 well tissue culture treated polystyrene plates (50 μ l separately to 3 wells) that were previously blocked with StartingBlock (Thermo Fisher). Particle fluorescence was measured at 485 nm excitation/527 nm emission to assess concentration, followed by addition of 50 μ l Amplex Red fluorescent peroxidase substrate (Invitrogen) per well. After 10 minutes, Amplex Red fluorescence signal was measured at 544 nm excitation/590 nm emission. Calibration curves prepared from stock particle and biotinylated HRP (Invitrogen) solutions were used to convert the respective fluorescence intensities to the receptor density per area of particle (n_r) by assuming a 1:1:1 ratio of binding site to probe to HRP. Non-receptor functionalized particles incubated with the HRP probes were used as controls.

Flow cytometry was used to characterize 9.95 μ m particles using R-phycoerythrin (RPE)-conjugated probes. scFv samples were assessed using FITC-biotin at 0.5 μ M followed by RPE-conjugated Neutravidin at 10 μ g/ml. Biotinylated BSA particles were stained directly with RPE-conjugated

Neutravidin at 10 $\mu\text{g/ml}$ concentration. Incubations were performed for 1 hour, with the primary reaction at room temperature and secondary reaction at 4°C. All washes were performed using three rounds of centrifugation and resuspension in ice-cold PBS⁺. Fluorescence was assessed by flow cytometry using a FACsCalibur (BD Biosciences), and fluorescence intensity was calibrated to the equivalent number of soluble RPE molecules using Quantum RPE calibration beads (Bangs Labs). The receptor density per area of particle (n_r) was then determined by assuming 1:1:1 ratio of binding site to probe to RPE. Both non-functionalized and functionalized particles incubated with secondary reagent only were used as controls.

Measurement of Substrate Ligand Density. Fluorescein, VCAM-1, or free Neutravidin site-densities were assessed by ELISA using an HRP-conjugated anti-mouse IgG₁ antibody. For Neutravidin substrates, D-biotin treatment was followed by FITC-biotin at 100 nM to act as a probe for free biotin binding sites. Substrates were blocked with ice-cold StartingBlock (Thermo Fisher) for approximately 10 minutes, followed by incubation with ice-cold PBS containing anti-fluorescein or anti-VCAM-1 antibody (mouse IgG₁, 2 $\mu\text{g/ml}$, 0.5 ml) for 1 hour at 4°C. Substrates were then washed three times with ice-cold PBS and treated with identical incubation and wash sequences using HRP-conjugated anti-mouse IgG₁ monoclonal antibody (1:500 dilution, 0.5 ml). ELISA reaction was initiated by addition of 0.9 ml TMB Turbo chromagenic peroxidase substrate (Thermo Fisher) and was allowed to continue for 10 minutes at room temperature before quenching with 1 ml of 1 M sulfuric acid. Absorbance was measured at 450 nm using a plate reader and converted to ligand site density per area substrate (n_l) by assuming a 1:1:1:1 ratio of ligand to primary antibody to secondary antibody to HRP.

Transport-Reaction Model. The rate constant for particle attachment (k_A) was isolated from the attachment rate ($k_A C_w$) using a transport-reaction model previously described.¹ The model accounts for convective and diffusive transport phenomena and tracks the free and bound particle species throughout the flow chamber, and thus decouples adhesion phenomena and depletion of the bulk particle concentration near the reactive wall. The convective-diffusion equation governing particle transport

within the flow chamber and the relevant boundary conditions are given below in dimensionless form:

$$\frac{\partial \hat{C}}{\partial \tau} + P\varepsilon[\eta - \eta^2] \frac{\partial \hat{C}}{\partial \xi} = \varepsilon^2 \frac{\partial^2 \hat{C}}{\partial \xi^2} + \frac{\partial^2 \hat{C}}{\partial \eta^2} \quad (\text{S1})$$

$$\hat{C}(\tau, \xi = 0, \eta) = 1 \quad (\text{S2a})$$

$$\frac{\partial \hat{C}}{\partial \xi}(\tau, \xi = 1, \eta) = 0 \quad (\text{S2b})$$

$$\frac{\partial \hat{C}}{\partial \eta}(\tau, \xi, \eta = 1) = 0 \quad (\text{S2c})$$

$$\frac{\partial \hat{C}}{\partial \eta}(\tau, \xi, \eta = 0) = \frac{\partial \hat{B}}{\partial \tau}(\tau, \xi) = \delta_A \hat{C}(\tau, \xi, \eta = 0) \quad (\text{S2d})$$

The dimensionless variables are defined as follows

$$\hat{C} \equiv \frac{C}{C_0} \quad \hat{B} \equiv \frac{B}{C_0 H} \quad \xi \equiv \frac{x}{L} \quad \eta \equiv \frac{y}{H} \quad \varepsilon \equiv \frac{H}{L} \quad \tau \equiv \frac{tD}{H^2} \quad (\text{S3})$$

$$P \equiv \frac{6UH}{D} \quad \delta_A \equiv \frac{k_A H}{D}$$

where C is the free particle concentration, C_0 is the inlet concentration, x is the axial coordinate, y is the coordinate perpendicular to the axis, L is the chamber length, D is the particle diffusivity and U is the average fluid velocity. Particle diffusivity was calculated using the Stokes-Einstein calculation ($D = k_B T / 6\pi\mu R_p$, where $k_B T$ is the thermal energy, μ is the fluid viscosity, and R_p is the particle radius).

Comsol Multiphysics software was used to calculate finite-element solutions by employing the two-dimensional transient convection-diffusion application to account for bulk transport within the flow chamber and the weak form boundary application to incorporate the reaction at the adhesive boundary. Solutions utilized a one second time-step and were carried out for a total of 14 minutes to emulate binding experiments. Binding phenomena was tracked at discrete nodes placed at the stage positions observed during experiments, and those results were averaged. The attachment rate constant k_A was then determined by matching the model and experimental attachment rates. The dimensional and dimensionless parameter values used in model solutions have been reported elsewhere.¹

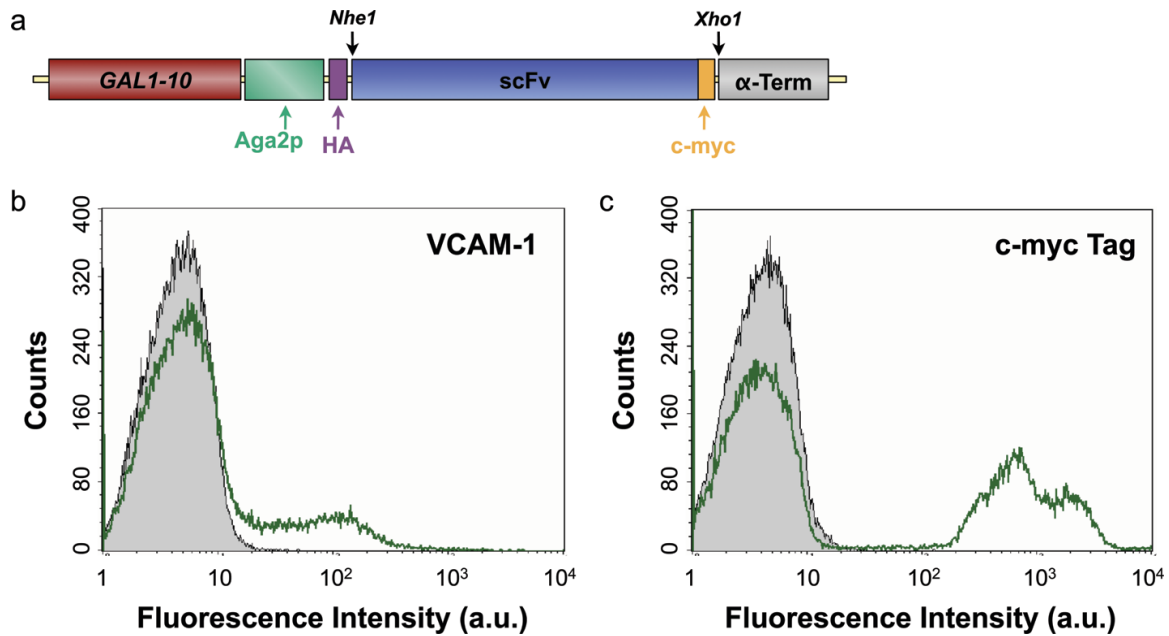


Figure S1: VIII scFv is expressed and binds VCAM-1. (a) Schematic representation of the yeast surface display expression cassette including GAL1-10 promoter, Aga2p protein to anchor the construct to the cell wall via linkage to Aga1p, scFv gene, c-myc epitope tag, and α -factor 3' untranslated region. (b and c) Flow cytometry results demonstrating scFv display using (b) functional VCAM-1 binding by treatment with VCAM-1/Fc chimaera and protein G-FITC and (c) indirect detection of the construct by treatment with anti-c-myc antibody. As typically observed for yeast surface display, bimodal staining was obtained due to the presence of a non-expressing population.² The second population was clearly positive in both assays, indicating that the full-length construct is expressed and the scFv binds VCAM-1.

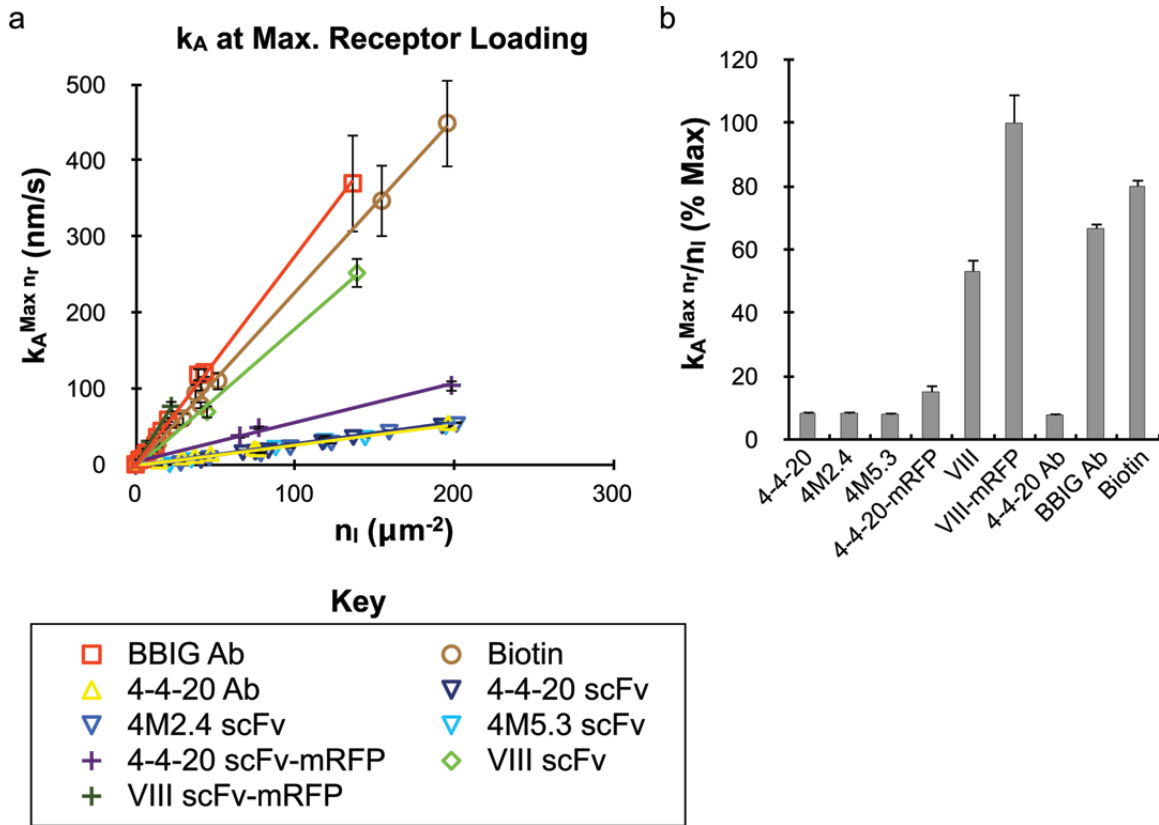


Figure S2: Nanoparticle attachment rate at the maximum receptor density. (a) Attachment rate (k_A) at the maximum receptor density plotted versus ligand density (n_l), showing that binding efficiency is comparable between the 4-4-20 scFv and full antibody. This is because the scFvs can be incorporated onto particles at much higher densities. Since addition of the mRFP protein does not affect nanoparticle loading but does improve binding efficiency, the 4-4-20 scFv-mRFP fusion outperforms the full 4-4-20 antibody. (b) Representation of the slope values ($k_A^{Max} n_r/n_l$) from part a for each binding interaction.

Table S1. Nanoparticle attachment and detachment rate parameters, presented per available adhesion molecule.

Receptor	Ligand	Attachment	Detachment		
		$k_A/n_r n_l$ ($\times 10^4 \text{ nm} \cdot \mu\text{m}^4/\text{s}$)	β	φ	$\kappa_D^0/n_r n_l$ ($\times 10^{-3} \mu\text{m}^{-4}\text{s}^{-1}$)
4-4-20 scFv	Fluorescein	0.14 ± 0.01	1.5	1	48.32 ± 17.10
4M2.4 scFv	Fluorescein	0.13 ± 0.01	1.5	1	25.54 ± 21.00
4M5.3 scFv	Fluorescein	0.13 ± 0.01	1.5	1	12.39 ± 3.54
4-4-20 scFv-mRFP	Fluorescein	0.27 ± 0.04	1.5	1	28.65 ± 33.20
4-4-20 Ab	Fluorescein	1.01 ± 0.08	1.5	1	3.83 ± 0.77
Biotin	Neutravidin	3.91 ± 0.12	1.5	1	0.57 ± 0.25
VIII scFv	VCAM-1	0.89 ± 0.07	$\frac{3}{4}$	1	2.07 ± 1.12
VIII scFv-mRFP	VCAM-1	1.67 ± 0.16	$\frac{3}{4}$	1	1.06 ± 0.28
BBIG Ab	ICAM-1	8.03 ± 0.23	$\frac{3}{4}$	$\frac{1}{3}$	0.10 ± 0.01

REFERENCES

- (1) Haun, J. B.; Hammer, D. A. *Langmuir* **2008**, *24*, 8821-8832.
- (2) Boder, E. T.; Wittrup, K. D. *Methods Enzymol* **2000**, *328*, 430-444.